Atmos. Chem. Phys. Discuss., 13, 9443–9483, 2013
www.atmos-chem-phys-discuss.net/13/9443/2013/
doi:10.5194/acpd-13-9443-2013

Atmospheric Chemistry and Physics Discussions
Open Access

NO_x cycle and tropospheric ozone isotope anomaly: an experimental investigation

G. Michalski, S. K. Bhattacharya, and G. Girsch

Department of Earth and Atmospheric Sciences and Department of Chemistry, Purdue University, 550 Stadium Mall Drive, West Lafayette, IN 47907, USA

Received: 16 January 2013 – Accepted: 18 March 2013 – Published: 11 April 2013

Correspondence to: G. Michalski (gmichals@purdue.edu)

Published by Copernicus Publications on behalf of the European Geosciences Union.

Abstract

The oxygen isotope composition of nitrogen oxides (NO_x) in the atmosphere may be a useful tool for understanding the oxidation of NO_x into nitric acid/nitrate in the atmosphere. A set of experiments were conducted to examine changes in isotopic composition of NO_x due to O_3-NO_x photochemical cycling. At low NO_2/O_2 mixing ratios, NO_2 becomes progressively and nearly equally enriched in ^{17}O and ^{18}O over time until it reaches a steady state with $\Delta^{17}O$ values of 40.6 ± 1.9 ‰ and $\delta^{18}O$ values of 84.2 ± 4 ‰, relative to the isotopic composition of the O_2 gas. As the mixing ratio increases, isotopic exchange between O atoms and O_2 and NO_x suppresses the isotopic enrichments. A kinetic model simulating the observed data shows that the isotope effects during ozone formation play a more dominant role compared to kinetic isotope effects during NO oxidation or exchange of NO_2. The model results are consistent with the data when the $NO + O_3$ reaction occurs mainly via the transfer of the terminal atom of O_3. The model predicts that under tropospheric concentrations of the three reactants, the timescale of NO_x isotopic equilibrium ranges from hours (ppbv mixing ratios) to days/weeks (pptv) and yields steady state $\Delta^{17}O$ and $\delta^{18}O$ values of 46 ‰ and 115 ‰ respectively with respect to Vienna Standard Mean Ocean Water. Interpretation of tropospheric nitrate isotope data can now be done with the derived rate coefficients of the major isotopologue reactions at various pressures.

1 Introduction

The NO_x cycle is the key driver of tropospheric chemistry (Monks et al., 2009; Seinfeld and Pandis, 1998) and the stable isotope composition of NO_x may be a useful tool for deciphering oxidation mechanisms occurring during photochemical cycling (Michalski et al., 2003; Morin et al., 2008; Savarino et al., 2008). Multiple oxygen isotope analysis is particularly useful for understanding oxidation chemistry because the original isotope signature of NO_x inherited from diverse sources are quickly erased due to rapid cycling of oxygen in the NO_x system. There are, however, no oxygen isotope measurements of in situ NO_x because it is reactive, has low mixing ratios (in the range of pptv to ppbv), and it would be prone to reacting with water when concentrated by collection devices. Atmospheric nitrate, which is the main end product of NO_x oxidation chemistry, has remarkable oxygen isotopic variations, including elevated $\delta^{18}O$ (Elliott et al., 2009; Hastings et al., 2003) and $\Delta^{17}O$ values (Michalski et al., 2003; Morin et al., 2008; Savarino et al., 2008), which suggests occurrence of interesting isotope effects during NO_x cycling. Variations in atmospheric nitrate $\Delta^{17}O$ values have been used to evaluate the relative importance of O_3 oxidation of NO and N_2O_5 heterogeneous reactions that form HNO_3. If proposals to use nitrate isotopic compositions as a way of inferring changes in oxidation chemistry in the modern (Michalski et al., 2003; Morin et al., 2008) or ancient atmosphere using ice cores nitrate (Alexander et al., 2004; Kunasek et al., 2008) are to be implemented, we need a better understanding of the interacting role of the various isotopologues involved in the reactions known as the Leighton cycle (Finlayson-Pitts and Pitts Jr., 2000; Leighton, 1961).

The Leighton reactions refer to the closed photochemical cycling of NO-O_2-O_3-NO_2 in the atmosphere. It is initiated when NO_2 is photolyzed by UV-visible light in the blue region of the spectrum (< 400 nm) yielding a ground state oxygen atom (O^3P). The main fate of the oxygen atom is to combine with O_2 to form O_3, which then oxidizes NO back to NO_2 (Finlayson-Pitts and Pitts Jr., 2000; Leighton, 1961):

$$NO_2 + h\nu \rightarrow NO + O^3(P) \tag{R1}$$

$$O^3(P) + O_2 \rightarrow^* O_3 \tag{R2}$$

$$^*O_3 + M \rightarrow O_3 + M \tag{R3}$$

$$O_3 + NO \rightarrow NO_2 + O_2 \tag{R4}$$

The intimate coupling between NO_x and O_3 expressed by the above reactions is believed to be the driver of the high $\delta^{18}O$ and $\Delta^{17}O$ values observed in atmospheric nitrate which overrides other oxidation channels (Michalski et al., 2003; Morin et al.,

ACPD
13, 9443–9483, 2013

2008; Savarino et al., 2008). The usual definition of δ in parts per thousand (‰) is used here $\delta^{18}O$ (‰) = $(R_{sam}/R_{ref} - 1) \cdot 1000$, where R_{sam} and R_{ref} denote the $^{18}O/^{16}O$ ratio in the sample (final) and reference (initial) respectively. $\Delta^{17}O$ value is the ^{17}O excess found in a compound over what is expected based on its $\delta^{18}O$ value. Assuming the rule of mass dependence in the two oxygen isotope ratios in its simple linearized form we can write: $\Delta^{17}O = \delta^{17}O - 0.52 \cdot \delta^{18}O$ (Miller, 2002). Ozone produced by photolysis and discharge experiments has $\delta^{18}O$ values enriched by 80–120 ‰ relative to the parent oxygen reservoir from which it is produced (Janssen et al., 2003; Mauersberger, 1981; Morton et al., 1989) as well as high $\Delta^{17}O$ values (~ 30-50 ‰)(Thiemens and Heidenreich III, 1983; Thiemens and Jackson, 1987; Thiemens and Jackson, 1990). This has been attributed to isotopic selectivity during the recombination Reactions (R2–R3) due to limitation imposed by symmetry properties of the heavy ozone molecule (Gao and Marcus, 2001; Hathorn and Marcus, 1999; Michalski and Bhattacharya, 2009). Some measurements of the $\delta^{18}O$ and $\Delta^{17}O$ value of O_3 in the troposphere (Johnston and Thiemens, 1997; Krankowsky et al., 1995) are similar to laboratory measurements, but most fall below the expected value (Johnston and Thiemens, 1997; Krankowsky et al., 1995; Vicars et al., 2012).

High $\delta^{18}O$ and $\Delta^{17}O$ values can be generated in NO_x and NO_y compounds when ozone transfers one of its oxygen atoms in Reaction (R4) to the NO_y products (Savarino et al., 2008). It has been hypothesized that NO-O_3-NO_2 photochemical cycling results in NO_x becoming enriched in the heavy oxygen isotopes through ozone in the intermediate oxidation step (Michalski et al., 2003; Morin et al., 2008). However, in view of the large number of possible reactions that can take place (e.g. photolysis, oxidation and isotope exchange) among the isotopologues of O_2, O_3, NO and NO_2 a quantitative laboratory study of the heavy isotope transfer from O_3 to NO_x is required. Here we address this issue for the first time by conducting a series of controlled photolysis experiments and assess the isotopic enrichment in NO_2 as a function of time and partial pressures of O_2 and NO_2.

ACPD
13, 9443–9483, 2013

2 Experimental procedure

A cylindrical photolysis chamber with associated vacuum extraction system was used for the present experiments. The chamber was 122 cm in length and 17 cm in diameter, made of Pyrex (~ 21 L) and fitted with a 6 cm diameter quartz window at one end. A 150 watt xenon solar simulator (PTI Photon Technology International, Ushio bulb model UXL 151H) having maximum output of 3000 lumens was used as the light source. The lamp has minimal flux at wavelengths shorter than 300 nm which was further cut off by the quartz window. It emits brightly in the visible region and its spectral flux in the 300–400 nm range (NO_2 has dissociation maximum at 400 nm) simulate ground level actinic flux. The NO_2 gas used in the photolysis was produced in the laboratory by reacting NO (99 % pure) with excess O_2 (99.99 % pure) and then purifying the product NO_2 by cryogenic separation; it was stored in a 2 L Pyrex bulb wrapped by aluminum foil to prevent exposure to light. Aliquots of this NO_2 were isolated by trapping them in a U-trap (20 mL volume) using liquid nitrogen. After pumping away non-condensable gases the trap was warmed to room temperature and pure NO_2 was allowed to expand into the reaction chamber (roughly a 1000 : 1 chamber to trap volume ratio). Ultra high purity O_2 (99.999 %) was then introduced in to the chamber through the same U-trap (to flush out small amount of left over NO_2) until the desired pressure was reached (50 to 750 torr). Next, the xenon lamp was switched on and the lamp was aligned and focused such that its light entered the reaction chamber through the quartz window along the long axis of the cylindrical vessel. All experiments were conducted at room temperature (298 °K).

The first series of experiments (Set 1) examined the isotope effect that occurred when the time of illumination was varied at a fixed NO_2/O_2 ratio of 20×10^{-6}. In the second case (Set 2), the NO_2/O_2 mixing ratios were varied from 3.1×10^{-5} to 4.3×10^{-4} by altering the aliquot amount of NO_2 while the illumination time was kept constant (~ 60 min). The final set of experiments (Set 3) examined the effect of O_2 pressure variation on isotope partitioning. In each case, after the specified time, the light was

ACPD
13, 9443–9483, 2013

switched off and the vessel was kept in the dark for about 60 min to effect oxidation of the product NO by O_3 and O_2 gas in the chamber so that total product of NO_x is obtained as NO_2. We assume that during the final collection only trivial amounts of NO is left and accordingly this assumption is used when calculating the isotope ratios in the model. It is implicitly assumed that higher oxides of nitrogen are not produced significantly and can be neglected. For example, it is known that N_2O_3 is formed in reaction of NO and NO_2 but breaks down to NO and NO_2 again inducing isotopic exchange (Sharma et al., 1970). Therefore, we consider no significant net production of N_2O_3. NO_2 was collected by pumping the NO_2/O_2 mixture (~3 h) slowly though a spiral trap immersed in liquid nitrogen. The purified NO_2 was taken in a small trap and converted to N_2 and O_2 by electric discharge produced by a Tesla coil (Michalski et al., 2002; Bes et al., 1970). The O_2 fraction was separated from the N_2 fraction using 5A molecular sieve column cooled to 173 °K using alcohol slush. The O_2 isotope ratios were determined using a Thermo Delta-V isotope ratio mass spectrometer in dual inlet mode. The $\delta^{18}O$ and $\delta^{17}O$ of the tank O_2 used for photolysis experiments are −10.84 ‰ and −5.69 ‰ (relative to VSMOW) respectively; for the NO_2 gas these values are −2.26 ‰ and −1.25 ‰ as determined by the discharge method.

2.1 Set 1 experiment

Experiments in this set were designed to evaluate the time required for the NO_x cycle to achieve isotopic steady state under the applied photochemical conditions (Fig. 1). Photochemical steady state in the NO_x cycling (Reactions R1–R3) is well known under tropospheric conditions of atmospheric chemistry (Finlayson-Pitts and Pitts Jr., 2000; Leighton, 1961) by

$$[O_3]_{ss} = j_1[NO_2]/k_4[NO] \tag{R5}$$

ACPD
13, 9443–9483, 2013

where j_1 is the photolysis rate constant (s^{-1}) and k_4 is the rate constant of Reaction (R4). Initializing the $[O_3]$ and [NO] to zero and solving for the evolution of ozone, which is equal to NO, in the system over time yields (Seinfeld and Pandis, 1998)

$$[O_3]_{ss} = \frac{1}{2}\left\{\left[\left(\frac{j_1}{k_4}\right)^2 + \frac{4j_1}{k_4}[NO_2]_o\right]^{\frac{1}{2}} - \frac{j_1}{k_4}\right\} \quad \text{(R6)}$$

This steady state is shifted when NO_x is present at high mixing ratios because the O sink reaction

$$NO_2 + O \rightarrow NO + O_2 \quad \text{(R7)}$$

becomes important (Crutzen and Lelieveld, 2001) and reduces the O_3 production rate so that Reaction (R6) no longer holds. In the present case, for the Set 1 experiments (20 ppmv NO_2) the observed isotopic steady state is achieved on the order of 30 min (Fig. 1). When the NO_2 amount is higher (for example, ~240 ppmv) the photolytic supply of O-atom is faster and the steady state is expected to be achieved in less time as verified from the model (described later). Based on these considerations, we selected 1 h as the time for subsequent experiments which is a period sufficient for isotopic steady state to be achieved.

2.2 Set 2 and Set 3 experiments

The second set of experiments (Set 2) was designed to determine the change in the NO_2 isotopic composition after photochemical cycling as a function of NO_2 mixing ratio. This was achieved by varying NO_2 amount from 16.8×10^{-6} to 236.0×10^{-6} mole (µmole) while keeping the O_2 at 0.4 moles using a constant O_2 pressure of 500 torr (Table 1 and Fig. 2). In contrast, the last set of experiments (Set 3) was done by keeping the NO_2 amount fixed at ~20 µmole (in the 20L chamber) while changing the O_2 pressure from 50 to 750 torr (Table 2). The results are plotted in terms of NO_2 $\Delta^{17}O$ and $\delta^{18}O$ values as a function of O_2 pressure (Fig. 3).

ACPD
13, 9443–9483, 2013

3 Discussion and model predictions

Both the data sets show that the steady state $\delta^{18}O$ and $\Delta^{17}O$ values are a strong function of the NO_2/O_2 mixing ratio (Fig. 7). As the NO_2 mixing ratio decreases, the $\Delta^{17}O$ and $\delta^{18}O$ values increase until they are nearly constant when NO_2 mixing ratio reaches about 20 ppmv. The highest observed $\delta^{18}O$ values (relative to tank O2) are: 84.2 ±4 ‰ ($n = 3$) and corresponding $\Delta^{17}O$ values are: 40.6 ± 1.6 ‰ (Table 2). The system was not designed for mixing ratios lower than 20 ppmv because this would be well below the minimum sample size needed for isotope analysis by dual-inlet method. For example, we could not investigate typical troposphere ratios (∼ 10 ppbv) which would have resulted in only about 10 nano-mole of O_2 in the present system.

A qualitative analysis of the reaction kinetics showed that the key to understanding the two data sets (Set 2 and Set 3) is the exchange reactions between oxygen atoms and NO_x or O_2 (for simplicity we write: O=^{16}O, P=^{17}O and Q=^{18}O) :

$$QO + O \longleftrightarrow Q + OO \tag{R8}$$

$$QNO + O \longleftrightarrow ONO + Q \tag{R9}$$

$$NQ + O \longleftrightarrow NO + Q \tag{R10}$$

Analogous exchanges occur with the ^{17}O (P) isotopic species (Table 3). All three exchange rate constants are of similar magnitude (Anderson et al., 1985; Jaffe and Klein, 1966; Sharma et al., 1970) but the NO_x exchange rate constants are slightly larger than the rate for O-O_2 exchange, albeit with considerable uncertainties (Jaffe and Klein, 1966). Since the overall rate of exchange is proportional to concentration, isotopic exchange between NO_x and the bath O_2 gas via Reactions (R8–R10) is expected to be a strong function of mixing ratio.

We hypothesize that the high isotope enrichments, reflected in both the $\delta^{18}O$ and the $\Delta^{17}O$ values, occur when ozone oxidation of NO is faster than NO_x-O_2 isotopic exchange. Isotopic enrichments associated with the formation of ozone have been extensively studied (Mauersberger et al., 1999; Guenther et al., 1999; Mauersberger et

ACPD
13, 9443–9483, 2013

al., 2003; Thiemens, 1999). At temperature and pressure range of the present experiments, the recombination process should generate ozone of $\delta^{18}O$ values between 90–130 ‰ with $\Delta^{17}O$ values between 30–46 ‰ (Table 5; Mauersberger et al., 2003). Our hypothesis is that during oxidation of NO the oxygen isotopic enrichments in ozone are transferred to the product NO_2. The enrichment in the product NO_2 is diluted or even erased when NO_x and O atoms exchange is fast via (R9) and (R10). This is because O_2 dominates as the oxygen reservoir in the present system (by about four orders of magnitude compared to ozone or O-atom) and O atoms produced by NO_2 photolysis quickly equilibrate with the O_2 bath gas via (R8). The equilibrated oxygen atom loses the heavy isotopic signal that arises from the (R2) and (R3). Therefore, there is a competition between the NO_x-O atom exchange and the oxidation by O_3. Typical number densities (molecules cm^{-3}) at the end of 60 min for 20 µmole of initial NO_2 are shown in Table 3 (values are from model run discussed later): this shows that after 60 min the O_3 concentration is higher by a factor of 100 for 750 torr compared to 50 torr O_2 pressure. On the contrary, the O-atom concentration is lower. This means that at 750 torr the NO oxidation by O_3 dominates over exchange by a factor of ten and correspondingly a 10 fold higher $\Delta^{17}O$ value is observed in the product NO_2 compared to the 50 torr case. In contrast, if we compare 750 torr O_2 and 236 µmole NO_2 case we note that the O_3 concentration has gone down by 44 %. This has the effect of reducing the $\Delta^{17}O$ in NO_x. This example shows that NO_2/O_2 ratio determines the net $\Delta^{17}O$ in NO_x under these experimental conditions. The $\Delta^{17}O$ values decrease with increase in NO_2/O_2 ratio but the nature of decrease is different for different O_2 bath pressure (see Fig. 4 along with Table 1 and Table 2).

Plotting oxygen isotope enrichments in dual isotope ratio space supports the hypothesis that NO_x cycling effectively equilibrates NO_x with O_3 (Fig. 5a, b and c). Two lines in Fig. 5a refer to two cases: Case 1 are data points obtained by changing the NO_2 amount from 20 to 236 µmole (variable NO_2) while keeping the oxygen pressure constant at 50 torr. Case 2 correspond to when NO_2 is kept constant at 20 µmole while the O_2 pressure is changed from 50 to 750 torr (variable pressure of O_2). The $\delta^{17}O$

ACPD
13, 9443–9483, 2013

NO_x cycle and tropospheric ozone isotope anomaly

G. Michalski et al.

and $\delta^{18}O$ data in both cases align nearly along a line of slope 1 reflecting the progressive transfer of ozone isotopic ratios to NO_2. Case 2 points reflect the same slope and intercept as obtained experimentally by earlier workers (Mauersberger et al., 2003) and shown in Fig. 5b. Figure 5c shows all NO_2 points plotted together where the best fit line has a slope of nearly unity and intercept −2.58. The observed NO_2 isotopic equilibrium values, when the NO_x-O exchange is minimized (i.e., ~20 ppmv and O_2 pressure at 750 torr), yields $\Delta^{17}O$ values of 40.6 ± 1.9 ‰ and $\delta^{18}O$ of 84.2 ± 4 ‰. The corresponding values expected for bulk ozone enrichment at 750 torr are 31.1 and 90.4 ‰ (Table 6). We note that the enrichment observed in NO_2 is thus approximately reflecting the expected isotope enrichment in ozone (discussed below). Unfortunately, the ozone could not be measured directly for its isotopic composition due to a very low amount (~0.2 to 20 nmole) mixed in large quantity (~4.0×10^5 µmole) of bath gas O_2. The NO_2 data suggests enrichment values in ozone are not different whether or not the oxygen atom is supplied by NO_2 dissociation via lower energy photons, or by high energy dissociation of O_2, (UV photolysis/electron impact). Therefore, in the ozone isotope enrichment process the initial energy distribution in O-atoms does not have any significant effect on the mass independent fractionation (MIF) of ozone.

We note that at steady state (with 750 torr O_2 and ~20 µmole NO_2, see Table 2), the NO_2 $\Delta^{17}O$ values (~40.6 ‰) are higher than those expected from bulk O_3 (O_3 ~31 ‰) whereas the $\delta^{18}O$ values are only slightly lower (O_3 ~90 ‰). This can be qualitatively explained by the isotopic distribution within the O_3 molecule and dynamical considerations of the NO + O_3 reaction. The MIF effect and a significant portion of the mass dependent isotope effect in O_3 occur because of symmetry restrictions (Gao and Marcus, 2001; Hathorn and Marcus, 1999; Heidenrich and Thiemens, 1986; Michalski and Bhattacharya, 2009). Isotopically homogenous O_3 ($^{16}O_3$) has C_{2v} symmetry, but when the terminal atoms are isotopically substituted the symmetry is reduced to C_s. Currently accepted phenomenological theory (Gao and Marcus, 2001; Hathorn and Marcus, 1999) surmises that this reduction in symmetry gives excited C_s-type ozone intermediates a longer lifetime due to increase in the number of allowed vibrational

ACPD
13, 9443–9483, 2013

couplings, which facilitates intermolecular energy redistribution. This extended lifetime gives the asymmetric O_3 species a higher probability of being quenched (R3) by a third body (M) relative to the symmetric species, which more readily undergoes unimolecular decomposition back to O + O_2. The result is that all of the $\Delta^{17}O$ enrichment and a significant portion of the $\delta^{18}O$ enrichment are located in the terminal atoms of the triangular O_3 molecule (Michalski and Bhattacharya, 2009; Tuczon and Janssen, 2006). Hence, by isotope mass balance, the $\Delta^{17}O$ values of the terminal atoms should be 3/2 higher that the $\Delta^{17}O$ value of the bulk O_3. Additionally, ab initio and experimental data suggests that the NO + O_3 reaction occurs mainly through abstraction of terminal oxygen atoms of ozone (Peiro-Garcia and Nebot-Gil, 2002; Redpath et al., 1978; Savarino et al., 2008). Therefore, ignoring any mass independent or mass dependent isotope effects in the NO_x cycling other than isotopic transfer from ozone to NO_x it can be approximated that at standard temperature and pressure the steady state NO_2 $\Delta^{17}O$ values would be 1.5 × 31 ‰ ∼ 46 ‰, slightly higher (∼ 5 ‰) than our observed value of ∼ 41 ‰. Part of this small discrepancy can be explained by the NO_x-O exchange still occurring at 20 ppmv NO_x/O_2 mixing ratio. The second possibility is that a fraction of the NO and O_3 reactions are occurring through abstraction of the central oxygen atom in ozone (Redpath et al., 1978; Vandenende et al., 1982; Vandenende and Stolte, 1984). In this case the 1.5 factor used to scale the bulk ozone isotope ratios would be too high. Savarino et al. (2008) performed a single step oxidation experiment of NO by O_3 to derive a conversion formula, which would give NO_2 $\Delta^{17}O$ values (38 ‰) slightly less than than our observed value.

3.1 Chemical kinetics modeling

In order to quantitatively interpret the observed NO_2 isotope values and evaluate the rate constants of the various reactions a chemical kinetic model was used that simulates isotope effects that occur during the photochemical cycle involving all possible isotopologues in the chamber (Table 5). We used a model called *kintecus* (Ianni, 2003)

Discussion Paper | Discussion Paper | Discussion Paper | Discussion Paper |
ACPD
13, 9443–9483, 2013
NOx cycle and tropospheric ozone isotope anomaly
G. Michalski et al.

and modified it for application to the present isotope system. The initial isotopologue reactants, the forward and backward reactions between various isotopologues along with their rate constants are supplied as inputs. The rate equations are solved numerically and the products are accumulated dynamically as the system evolves up to a pre-specified period (60 min in the present case). The model calculates the number of molecules of a pre-specified set of reactants at small intervals and finally displays the results in an excel file format at suitable time intervals.

3.2 Reactants, their initialization and delta definition

In the present case the model is initialized with the following 17 species (for simplicity we use: P = ^{17}O, Q = ^{18}O) O, P, Q, OO, OP, OQ, ONO, PNO, QNO, NO, NP, NQ, OOO, OQO, OOQ, OPO, and OOP. Note that we neglect to differentiate between ^{15}N and ^{14}N since the N- isotopes are not of our concern in these experiments. We also do not include minor species like PP or QQ or QQQ etc. since the probability of two or more minor isotopes reacting is small because of their low natural abundances. This neglect causes a minor problem of isotope balance since, in reality, all possible reactions involving all possible isotopologues occur in the reaction chamber and they affect the final abundances of the species. Obviously, the heavy isotopes distributed among the neglected species are not accounted for in the calculation of final delta values. However, this approximation results in model predictions that differ only slightly (less than 0.1 ‰) from the values if the minor isotopologues were included. For example, when we estimate isotope ratio Q/O in oxygen from molecular species ratio [OQ]/{2*[OO]+[OP]+[OQ]} disregarding contribution from QQ isotopologue the true ratio Q/O is underestimated by only about 2.4 ppt. Following the above restriction we define the isotope ratios of O_3, NO_2 and NO in the model as follows:

For oxygen $Q/O = [OQ]/\{2*[OO]+[OP]+[OQ]\}$

$$P/O = [OP]/\{2*[OO]+[OP]+[OQ]\}$$

ACPD
13, 9443–9483, 2013

NO$_x$ cycle and tropospheric ozone isotope anomaly

G. Michalski et al.

$$\text{For } O_3 \quad P/O = \{[OOP]+[OPO]\}/\{3[OOO]+2[OOQ]+2[OQO]+2[OOP]+2[OPO]\}$$

$$Q/O = \{[OOQ]+[OQO]\}/\{3[OOO]+2[OOQ]+2[OQO]+2[OOP]+2[OPO]\}$$

$$\text{For } NO_2 \quad P/O = [PNO]/\{2\cdot[ONO]\}$$

$$Q/O = [QNO]/\{2\cdot[ONO]\}$$

$$\text{For NO} \quad P/O = [NP]/[NO]$$

$$Q/O = [NQ]/[NO]$$

At the beginning of the simulation only isotopologues of NO_2 and O_2 are present in the chamber. The initial amounts of species OO, OP and OQ as well as ONO, PNO and QNO (Table 4) are chosen such that the δ values (relative to VSMOW) of tank O_2 and starting NO_2 agree with the measured ones according to the above definitions. The delta-values (relative to VSMOW) are converted to molecular abundances using the isotopic abundances of O, P and Q of VSMOW (Table 4) obtained from Coplen et al. (2002). As mentioned, the kintecus output results are displayed in terms of number of molecules of various isotopologue species (e.g., OOO, OQO or OOQ). These are converted to δ values (or enrichment) relative to the tank O_2. The enrichment values act as anchor points since the correctness of the numerical results is ensured by comparing the calculated ozone δ values with experimental ozone isotopic enrichment values obtained from pressure dependence studies of Guenther et al. (1999) and Mauersberger et al. (2003). It is to be noted that for application to troposphere the enrichment values can be converted to δ values relative to VSMOW by using the air oxygen isotope values (23.5 and 12.2 ‰ relative to VSMOW).

3.3 Choice of kinetic rate constants

Once initialized the simulation begins producing isotopologues of secondary reactants based on rate laws and constants (in units of $cm^3\,s^{-1}$ for bimolecular reactions and $cm^6\,s^{-1}$ for tri-molecular case) as listed in Table 5. Rate constants of NO oxidation by

ACPD
13, 9443–9483, 2013

O-atom and ozone are taken from the JPL listing as is the rate for reaction O + ONO. The rates for all reactions involving isotopologues (either in dissociation or bi-molecular reactions) were adjusted for the reaction channel symmetry. For example, reaction rate of the reaction PNO → P + NO rate constant is derived from the ONO → O + NO rate constant divided by two. For reactions Q + ONO and P + ONO the collision frequency factors of 0.957 and 0.978 were used (following the method of Pandey and Bhattacharya (2006) applied in the present case). Rate constants that produced the minor oxygen isotopologues of nitrogen oxides and where no experimental data is available were assumed to be the same as the major isotopic species (i.e., ignoring any kinetic isotope effect – KIE).

The NO_x exchange reaction rate constants were taken from published works. The forward exchange rate (k_f) of Q isotope with ONO is based on Jaffe and Klein (1966). For backward exchange rate (k_b) we used the equilibrium constant (K_{eq}) of Richet et al. (1977) such that at equilibrium (at temperature 298 K) the fractionation factor is given by the ratio $K_{eq} = k_f/k_b$ (Richet et al., 1977). Similar considerations were used for P + ONO exchange as discussed in Pandey and Bhattacharya (2006). In a similar way, exchange rates of O-atoms with NO were derived using Anderson et al. (1985) and Richet et al. (1977). Finally, the NO oxidation by bath gas O_2 was taken from Finlayson and Pitts (2000). For completeness, we included exchange of NQ with ONO and NP with ONO using the rate constant given by Lyons (2001). A rate coefficient for NO_2 dissociation that reproduced the time dependent isotopic equilibration data (Fig. 2) was 0.004 s^{-1} and this was used as the coefficient for all NO_2 isotopologues corrected for channel symmetry factor. The model does not distinguish between the two N-isotopes and it also assumes that only terminal atoms react when considering reactions or dissociation of tri-atomics.

3.4 Ozone formation rates and dissociation rates

The rate constants of ozone formation are the crucial part of the reaction scheme because in these reactions the mass independent isotopic enrichment arises and is then transferred to NO_x by mass dependent reactions. The ozone formation rates at low pressure (~ 50 torr) were mostly taken from Janssen et al. (2001). For the OOP case the relation between zero point energy change and rate constant ratios (Janssen et al., 2001) was used (See discussion in Bhattacharya et al., 2008). We note that out of the nine rate constants only the rates of O + OQ → OOQ and O + OP → OOP are surprisingly large and these are the reactions that essentially determine the level of MIF in ozone (Guenther et al., 1999; Janssen et al., 1999). We shall assume that the observed pressure dependence of ozone MIF is *due only to the variation in these two rates*. This hypothesis is based on the observation of Janssen et al. (1999) that O + OQ → OOQ is the channel which "almost exclusively is responsible for the observed enrichment in $^{50}O_3$". With this proviso, the present model can be used to find the pressure dependence of these two rate coefficients (denoted as r^{18} and r^{17}) relative to the rate of O + OO → OOO by fitting the modeled $\Delta^{17}O$ of NO_2 with the observed values. There is another constraint in this fitting, namely, the model δ values of ozone at various pressures must match the data on pressure variation given by Guenther et al. (1999) and Mauersberger et al. (2003). We found that it is possible to obtain consistent set of rate constants (given in terms of r^{18} and r^{17} values and shown in Table 6) for various pressures which satisfy both the ozone MIF data and our observed $\Delta^{17}O$ data of NO_2.

The ozone amount at any stage is quite small (O_3/NO_2 ratio is about 3×10^{-4} at 20 µmole of NO_2) but for proper calculation of the isotope effect one has to account for ozone dissociation. The rate constants of dissociation of various ozone isotopologues were taken from Pandey and Bhattacharya (2006) and Chakraborty and Bhattacharya (2003) normalized to the rate for the main ozone isotopologue $^{16}O^{16}O^{16}O$ which was fixed by taking the cross section ratio of NO_2 and O_3 at the wave-length range used for the experiment. This set of reactions being mass dependent in nature does not have significant effect on the $\Delta^{17}O$ of NO_2 as expected

ACPD
13, 9443–9483, 2013

3.5 Accounting for isotopes of total NO_x

The outcome of the model shows that at the end of each exposure period there are some NO molecules present. After the light source is switched off these NO molecules are expected to be quickly converted to NO_2 by oxidation by the remaining ozone or the O_2 bath gas, thus the assumption that the liquid nitrogen trap collects only NO_2. This process is not accounted for in the model because it does not have the provision to turn off the photon flux at a specified time during the simulation. This limitation has to be properly accounted for when calculating the model δ values so that they can be compared to the observations. The δ value of final NO_2 is a mixture of NO_2 at photo-stationary state plus NO_2 produced by NO oxidation after the light has been turned off. This is given by:

$$\delta NO_2 = x \cdot \delta(NO_2) + (1 - x) \cdot [m(\delta NO + \delta O_2)/2 + n(\delta NO + \delta O_{3t})/2] \quad (1)$$

where $\delta = \delta^{18}O$ or $\Delta^{17}O$, x and $(1 - x)$ are the mole fraction of NO_x as NO_2 and NO respectively at the instant the light is turned off and m and n are the mole fractions of NO oxidized by molecular oxygen and ozone (through its terminal position atom denoted by O_{3t}) in the dark. Given the disparity in reaction rates constants for NO oxidation by O_2 and O_3, it is approximated that n = [OOO]/[NO] and m = {[NO] – [OOO]}/[NO]. In the model n varies in a small range from 0 to 0.009 since the ozone amount at any instant is quite small compared to the NO amount.

The observed isotope values in NO_2 were used to constrain the ozone rate constants in the model, which are then compared to previous works. First, the rate coefficients for reactions O + OQ + M → OOQ + M and O + OP + M → OOP + M (or the factors r^{18} and r^{17} to be multiplied respectively with the rate of O + OO + M → OOO + M; see Table 5) were selected that would reproduce closely the δ values reported by Guenther et al. (1999) and Mauersberger et al. (2003) for pressures 50, 75, 100, 150, 200, 300, 400, 500, 600, 700, and 750 torr of O_2. The kintecus model was run for this while keeping the NO_2 amount at 20 µmole. As an example, at a pressure of 50 torr the chosen

ACPD
13, 9443–9483, 2013

values are: $r^{18} = 1.450$ and $r^{17} = 1.335$ (Table 6). The 60 min kintecus simulation results in ozone δ^{18}O and δ^{17}O values of 128.0 ‰ and 112.5 ‰ which match exactly the estimates based on data given by Guenther et al. (1999). The predicted Δ^{17}O value of NO_2 for this case is 2.6 ‰ which compares well with the observed value 2.9 ‰ (Table 2). Similar comparisons can be done between modeled ozone δ values and literature based values mentioned above and are shown in Table 4. There is good agreement between the two sets of values. The differences are smaller than 0.8 ‰ for both δ^{18}O and δ^{17}O (Fig. 6) and 0.5 ‰ for Δ^{17}O values of O_3. We should mention here that the experimental values reported by Guenther et al. (1999) and Mauersberger et al. (2003) have large dispersion in some ranges and we used smooth fit to the data points to estimate the enrichments at specified pressure values (Table 6). Additionally, they refer to the photolytically produced ozone δ values in an oxygen-nitrogen system whereas the model values refer to ozone where the O-atoms are supplied by NO_2 dissociation and can exchange with O_2, NO and NO_2 and the ozone reacts with NO and NO_2. The rate constant values obtained by this fitting technique and given in Table 6, therefore, may have some limitation in application to a pure O_2-N_2 environment pertaining to laboratory ozone experiments. But they should be appropriate in case of atmospheric applications.

The Δ^{17}O values of NO_2 predicted by the model for the chosen experimental conditions are given in Table 1 (experiment set 2) and Table 2 (for experiment set 3) along with the experimental values. On the whole there is good agreement between the observed Δ^{17}O values and those derived by the model for both the sets (compare columns 7 and 10 in Table 1 and columns 8 and 11 in Table 2). The two sets agree on average within 1 ‰. Both sets show a decrease in the Δ^{17}O value of NO_2 with increase in the ratio NO_2/O_2 and the model values also reproduce this feature quite well (Fig. 4). It is clear that there is opposing effect of oxygen pressure (or amount) and NO_2 amount on the Δ^{17}O value of NO_2. As the O_2 pressure increases the ozone formation rate increases. For example, the kintecus output shows that for increase of pressure from 100 torr to 700 torr the average ozone formation rate increases from 1.0×10^{11} to

ACPD
13, 9443–9483, 2013

2.1×10^{12} (molecules s^{-1}). This increase results in enhanced ozone oxidation of NO and subsequently a larger $\Delta^{17}O$ values in NO_2 as qualitatively discussed above. When the amount of NO_2 increases at a fixed O_2 pressure the ozone formation rate is constant but the exchange of O-atom with NO_2 increases which reduces the $\Delta^{17}O$. It is therefore clear that when the original reservoir of NO_2 is large any effect introduced by the ozone oxidation step would be relatively small compared to the case when the NO_2 reservoir is smaller. The effect of each of these reactions can be explored by the kintecus model quantitatively.

The good agreement between the results with the model predictions and the observations allow us to propose variations of factors r^{17} and r^{18} with pressure of oxygen (Table 6 and Fig. 7). There is decrease in both these factors with increasing pressure consistent with the observed decrease in MIF of ozone at high pressure. The decrease for r^{18} is from 1.450 to 1.330 for a pressure increase from 50 to 750 torr. We can speculate in the light of Gao-Marcus model that the main reason for this decrease is an increase in collision frequency which lowers the life time of the transition state of the asymmetrical ozone isotopomer (known to be the factor responsible for MIF). This factor causes large change in asymmetrical ozone abundance as expected. For example, at 50 torr the O_3 $\delta^{18}O$ values (in ‰) are: 150 (asymm) and 85 (symm) whereas at 750 torr the values are 93 (asymm) and 85 (symm). Correspondingly, the modeled $\Delta^{17}O$ of bulk ozone changes from 46 to 31 ‰.

3.6 Atmospheric applications

Since the experimentally validated model results are based only on isotopologue rate constants (independent of mixing ratios) the model can be used to predict the expected oxygen isotope composition of NO_x in the atmosphere. NO_x mixing ratios vary widely in the atmosphere depending on the proximity to NO_x sources; urban regions are typically 10's of ppbv, while remote ocean regions can be as low as 10 pptv. For standard temperature and pressure, the model predicts the same steady state NO_2 $\Delta^{17}O$ and

$\delta^{18}O$ values (with respect to VSMOW), 46 ‰ and 115 ‰ respectively, regardless of mixing ratio over the range of 10 pptv to 10 ppbv. It is unlikely tropospheric ozone sourced from the stratosphere would impact the predicted isotope values in NO_x even in remote regions. Remote tropospheric ozone mixing ratios are often dominated by cross tropopause mixing of stratospheric ozone and this ozone would have an isotopic composition that reflects the stratospheric pressure and temperature conditions of its formation. However, this influence is expected to be minor because while the chemical lifetime of ozone in a clean troposphere may be months, the isotopic lifetime would be much less. Ozone photolysis and reformation in the troposphere would reset its isotopic composition, and this recycling rate is limited by ozone's photolysis lifetime of $\tau = 1/j_{O_3}$ Ozone j coefficients in the troposphere vary depending on the overhead total ozone column, latitude, time of day, and other phenomena that change photon fluxes, but have a daily average $\sim 1 \times 10^{-4}\,s^{-1}$ ($\tau \sim 3$ h). Thus in less than a day any stratospheric O_3 transported to the troposphere would have its isotope composition reset to values based on $T-P$ of the air mass in which it photolyzes and reforms.

While the isotopic equilibrium value is the same regardless of NO_x mixing ratios, the timescale to reach isotopic equilibrium is significantly different (Fig. 7). In urban to rural conditions (1–10 ppbv) equilibrium is reached within a few hours, but in pristine environments it may take from days to over a week for NO_x to reach isotope equilibrium. This longer equilibrium time predicted by the model is likely an overestimation because at ppbv levels in a NO_x only system NO = O_3 which makes the cycling rate significantly slower. In the real world, even in remote regions of the troposphere, 10 pptv levels of O_3 are rare, and are they typically 5 times higher than NO_x (Crutzen and Lelieveld, 2001; Faloona et al., 2000; Jaegle et al., 2000; Liu et al., 1987), which would accelerate the equilibrium process. The timescale to $\Delta^{17}O$ equilibrium would not likely be sensitive to alternate NO oxidants in clean environments. Under low NO_x conditions, hydroperoxy and organo-peroxy radicals are the main oxidants that convert NO into NO_2. But, these radicals form mainly when H and organic radicals (R) react with air O_2, which has a $\Delta^{17}O$ value of about zero and by extension these values would be similar in the

ACPD
13, 9443–9483, 2013

NO$_x$ cycle and tropospheric ozone isotope anomaly

G. Michalski et al.

product peroxy radicals, ignoring mass-dependent KIEs. Oxidation of NO by HO_2 and RO_2 should also follow mass dependent isotope rules; so NO_2 produced during peroxy radical oxidation should have a $\Delta^{17}O$ value of zero. Therefore, peroxy radical may alter the final $\Delta^{17}O$ value based on the proportion of peroxy radical oxidation relative to O_3 oxidation (Michalski et al., 2003; Morin et al., 2004), but it would not impact the timescale to reach $\Delta^{17}O$ equilibrium because the rate limiting step is the O_3 oxidation (unless there was no O_3 oxidation). The lifetime for conversion of NO_2 into HNO_3 by reaction by hydroxyl radical is on the order of 10 h so there may be situations in remote regions where NO_x does not reach isotope equilibrium before being converted to nitric acid. This would lead to low $\Delta^{17}O$ and $\delta^{18}O$ values in the product nitrate.

4 Conclusions

The isotope systematics of the NO_x cycle have been investigated experimentally and through kinetic modeling. The experiments confirm that photochemical cycling between NO_x and ozone generate high $\delta^{18}O$ and $\Delta^{17}O$ values in NO_x as the rapid photochemical cycling effectively equilibrates O_3 and NO_x. The good agreement between the predictions of the model that uses literature experimental rate constants and the observations suggests the NO oxidation by O_3 occurs primarily through the terminal atom extraction as predicted by ab initio calculations. The $\Delta^{17}O$ and $\delta^{18}O$ values of tropospheric NO_2 relative to VSMOW are estimated to be 46 ‰ and 115 ‰ based on this experimentally validated model.

Acknowledgements. We would like to thank the National Science Foundation for support NSF-AGS 0856274. Paul Shepson of Purdue University Dept of Chemistry for use of the Xenon lamp. SKB thanks Dept of Earth Sciences, Purdue University for hospitality. Sergie Oleynik for assistance in building the extraction system.

ACPD
13, 9443–9483, 2013

References

Alexander, B., Savarino, J., Kreutz, K. J., and Thiemens, M. H.: Impact of preindustrial biomass-burning emissions on the oxidation pathways of tropospheric sulfur and nitrogen, J. Geophys. Res., 109, D08303 doi:10.1029/2003JD004218, 2004.

Anderson, S. M., Klein, F. S., and Kaufman, F.: Kinetics of the Isotope Exchange-Reaction of ^{18}O with NO and O_2 at 298-K, J. Chem. Phys., 83, 1648–1656, 1985.

Bes, R., Lacoste, G., and Mahenc, J.: Mass spectrometric analysis of nitrogen and oxygen isotopes in nitrogen oxide compounds: electric glow discharge method Method. Phys. Anal., 6, 109–112, 1970.

Bhattacharya, S. K., Pandey, A., and Savarino, J.: Determination of intramolecular isotope distribution of ozone by oxidation reaction with silver metal, J. Geophy. Res., 113, D03303, doi:10.1029/2006JD008309, 2008.

Chakraborty, S. and Bhattacharya, S. K.: Oxygen isotopic fractionation during UV and visible light photodissociation of ozone, J. Chem. Phys., 118, 2164–2172, 2003.

Coplen, T. B., Bohlke, J. K., Bievre, P. D., Ding, T., Holden, N. E., Hopple, J. A., Krouse, H. R., Lamberty, A., Peiser, H. S., Revesz, K., and Rieder, S. E.: Isotopr abundance variationsof selected elements (IUPAC Technical Report), Pure Appl. Chem., 74, 1987–2017, 2002.

Crutzen, P. J. and Lelieveld, J.: Human impacts on atmospheric chemisty, Ann. Rev. Earth Plan. Sci., 29, 17–45, 2001.

Elliott, E. M., Kendall, C., Boyer, E. W., Burns, D. A., Lear, G. G., Golden, H. E., Harlin, K., Bytnerowicz, A., Butler, T. J., and Glatz, R.: Dual nitrate isotopes in dry deposition: Utility for partitioning NO_x source contributions to landscape nitrogen deposition, J. Geophys. Res., 114, D08303 doi:10.1029/2003JD004218, 2009.

Faloona, I., Tan, D., Brune, W. H., Jaegle, L., Jacob, D. J., Kondo, Y., Koike, M., Chatfield, R., Pueschel, R., Ferry, G., Sachse, G., Vay, S., Anderson, B., Hannon, J., and Fuelberg, H.: Observations of HO_x and its relationship with NOx in the upper troposphere during SONEX, J. Geophys. Res., 105, 3771–3783, 2000.

Freyer, H. D., Kley, D., Volz-Thomas, A., and Kobel, K.: On the interaction of isotope exchange processes with photo-chemical reactions in atmospheric oxides of nitrogen, J. Geophys. Res., 98, 14791–14796, 1993.

Finlayson-Pitts, B. J. and Pitts, Jr., J. N.: Chemistry of the Upper and Lower Atmosphere, Academic Press, San Diego, 2000.

Gao, Y. Q. and Marcus, R. A.: Strange and unconventional isotope effects in ozone formation, Science, 293, 259–263, 2001.
Guenther, J., Erbacher, B., Krankowsky, D., and Mauersberger, K.: Pressure dependence of two relative ozone formation rate coefficients, Chem. Phys. Lett., 306, 209–213, 1999.
Hastings, M. G., Sigman, D. M., and Lipschultz, F.: Isotopic evidence for source changes of nitrate in rain at Bermuda, J. Geophys. Res., 108, 4790, DOI:10.1029/2003JD003789, 2003.
Hathorn, B. C. and Marcus, R. A.: An intramolecular theory of the mass-independent isotope effect for ozone. I, J. Chem. Phys., 111, 4087–4100, 1999.
Heidenrich, J. E. and Thiemens, M. H.: A non-mass-dependent oxygen isotope effect in the production of ozone from molecular oxygen: the role of molecular symmetry in isotope chemistry, J. Chem. Phys., 84, 2129–2136, 1986.
Ianni, J. C.: KINTECUS, Vast Technologies Development Inc, Kintecus License Division 26, Willowbrook Avenue, Lansdowne, Pa 19050, 1995.
Jaegle, L., Jacob, D. J., Brune, W. H., and Wennberg, P. O.: Chemistry of HO_x radicals in the upper troposphere, Atmos. Environ., 35, 469–489, 2000.
Jaffe, S. and Klein, F. S.: Isotopic exchange reactions of atomic oxygen produced by the photolysis of NO_2 at 3660 °A, Trans. Faraday Soc., 62, 3135–3141, 1966.
Janssen, C., Guenther, J., Krankowsky, D., and Mauersberger, K.: Relative formation rates of $^{50}O(3)$ and $^{52}O(3)$ in $^{16}O^{18}O$ mixtures, J. Chem. Phys., 111, 7179–7182, 1999.
Janssen, C., Guenther, J., Mauersberger, K., and Krankowsky, D.: Kinetic origin of the ozone isotope effect: a critical analysis of enrichments and rate coefficients, Phys. Chem. Chem. Phys., 3, 4718–4721, 2001.
Janssen, C., Guenther, J., Krankowsky, D., and Mauersberger, K.: Temperature dependence of ozone rate coefficients and isotopologue fractionation in $^{16}O^{18}O$ oxygen mixtures, Chem. Phys. Lett., 367, 34–38, 2003.
Johnston, J. C. and Thiemens, M. H.: The isotopic composition of tropospheric ozone in three environments, J. Geophys. Res., 102, 25395–25404, 1997.
Krankowsky, D., Bartecki, F., Klees, G. G., Mauersberger, K., Schellenbach, K., and Stehr, J.: Measurement of heavy isotope enrichment in tropospheric ozone, Geophys. Res. Lett., 22, 1713–1716, 1995.
Kunasek, S. A., Alexander, B., Steig, E. J., Hastings, M. G., Gleason, D. J., and Jarvis, J. C.: Measurements and modeling of $\Delta^{17}O$ of nitrate in snowpits from Summit, Greenland, J. Geophy. Res., 113, D24302, doi:10.1029/2008JD010103, 2008.

ACPD
13, 9443–9483, 2013

Leighton, P. A.: Photochemistry of air pollution, Academic Press, New York, 1961.
Liu, S. C., Trainer, M., Fehsenfeld, F. C., Parrish, D. D., Williams, E. J., Fahey, D. W., Hubler, G., and Murphy, P. C.: Ozone production in the rural troposphere and the implications for regional and global ozone distributions, J. Geophys. Res., 92, 4191–4207, doi:10.1029/JD092iD04p04191, 1987.
Lyons, J. R.: Transfer of mass-independent fractionation in ozone to other oxygen-containing radicalsin the atmosphere, Geophys. Res. Lett., 28, 3231–3234, 2001.
Mauersberger, K.: Measurement of Heavy Ozone in the Stratosphere, Geophys. Res. Lett., 8, 935–937, 1981.
Mauersberger, K., Erbacher, B., Krankowsky, D., Gunther, J., and Nickel, R.: Ozone isotope enrichment: Isotopomer-specific rate coefficients, Science, 283, 370–372, 1999.
Mauersberger, K., Krankowsky, D., and Janssen, C.: Oxygen isotope processes and transfer reactions, Space Sci. Rev., 106, 265–279, 2003.
Michalski, G. and Bhattacharya, S. K.: The role of symmetry in the mass independent isotope effect in ozone., P. Natl. Acad. Sci., 1060, 11496–11501, 2009.
Michalski, G., Savarino, J., Böhlke, J. K., and Thiemens, M.: Determination of the total oxygen isotopic composition of nitrate and the calibration of a Δ^{17}O nitrate reference material Anal. Chem., 74, 4989–4993, 2002.
Michalski, G., Scott, Z., Kabiling, M., and Thiemens, M.: First Measurements and Modeling of Δ^{17}O in Atmospheric Nitrate, Geophys. Res. Lett., 30, 1870, doi:10.1029/2003GL017015, 2003.
Miller, M. F.: Isotopic fractionation and the quantification of ^{17}O anomalies in the oxygen three-isotope system: an appraisal and geochemical significance, Geochim. Cosmochim. Acta, 66, 1881–1889, 2002.
Monks, P. S., Granier, C., Fuzzi, S., Stohl, A., Williams, M. L., Akimoto, H., Amann, M., Baklanov, A., Baltensperger, U., Bey, I., Blake, N., Blake, R. S., Carslaw, K., Cooper, O. R., Dentener, F., Fowler, D., Fragkou, E., Frost, G. J., Generoso, S., Ginoux, P., Grewe, V., Guenther, A., Hansson, H. C., Henne, S., Hjorth, J., Hofzumahaus, A., Huntrieser, H., Isaksen, I. S. A., Jenkin, M. E., Kaiser, J., Kanakidou, M., Klimont, Z., Kulmala, M., Laj, P., Lawrence, M. G., Lee, J. D., Liousse, C., Maione, M., McFiggans, G., Metzger, A., Mieville, A., Moussiopoulos, N., Orlando, J. J., O'Dowd, C. D., Palmer, P. I., Parrish, D. D., Petzold, A., Platt, U., Pöschl, U., Prevot, A. S. H., Reeves, C. E., Reimann, S., Rudich, Y., Sellegri, K., Steinbrecher, R., Simpson, D., ten Brink, H., Theloke, J., van der Werf, G. R., Vautard, R., Vestreng, V., Vla-

ACPD
13, 9443–9483, 2013

NO_x cycle and tropospheric ozone isotope anomaly

G. Michalski et al.

chokostas, C., and von Glasow, R.: Atmospheric composition change – global and regional air quality, Atmos. Environ., 43, 5268–5350, 2009.
Morin, S., Savarino, J., Frey, M. M., Yan, N., Bekki, S., Bottenheim, J. W., and Martins, J. M. F.: Tracing the origin and fate of NO_x in the arctic atmosphere using stable isotopes in nitrate, Science, 322, 730–732, 2008.
Morton, J., Schueler, B., and Mauersberger, K.: Oxygen Fractionation of Ozone Isotopes $^{48}O(3)$ Through $^{54}O(3)$, Chem. Phys. Lett., 154, 143–145, 1989.
Pandey, A. and Bhattacharya, S. K.: Anomalous oxygen isotope enrichment in CO_2 produced from O+CO: estimates based on expeimental results and model predictions. J. Chem. Phys., 124, 234301, doi:10.1063/1.2206584, 2006.
Peiro-Garcia, J. and Nebot-Gil, I.: Ab initio study of the mechanism and thermochemistry of the atmospheric reaction NO + $O_3 \rightarrow NO_2 + O_2$, J. Phys. Chem A, 106, 10302–10310, 2002.
Redpath, A. E., Menzinger, M., and Carrington, T.: Molecular-Beam Chemiluminescence: Kinetic and internal energy dependence of $NO+O_3 \rightarrow NO_2^* \rightarrow NO_2 + h\nu$ reaction, Chem. Phys., 27, 409–431, 1978.
Richet, P., Bottinga, Y., and Javoy, M.: Review of hydrogen, carbon, nitrogen, oxygen, sulfur, and chlorine stable isotope fractionation among gaseous molecules, Ann. Rev. Earth Plan. Sci., 5, 65–110, 1977.
Sander, S. P., Friedl, R. R., Ravishankara, A. R., Golden, D. M., Kolb, C. E., Kurylo, M. J., Molina, M. J., Moortgat, G. K., Keller-Rudek, H., Finlayson-Pitts, B. J., Wine, P. H., Huie,R. E., and Orkin, V. L.: Chemical kinetics and photochemical data for use in atmospheric studies, Evaluation Number 15, JPL Publication 06-2, 2006.
Savarino, J., Bhattacharya, S. K., Morin, S., Baroni, M., and Doussin, J. F.: The $NO+O_3$ reaction: A triple oxygen isotope perspective on the reaction dynamics and atmospheric implications for the transfer of the ozone isotope anomaly, J. Chem. Phys., 128, 194303, doi:10.1063/1.2917581, 2008.
Seinfeld, J. H. and Pandis, S. N.: Atmospheric chemistry and physics : from air pollution to climate change, New York, Wiley, 1998.
Sharma, H. D., Jervis, R. E., and Wong, K. Y.: Isotopic exchange reactions in nitrogen oxides, J. Phys. Chem., 74, 923–933, 1970.
Thiemens, M. H.: Mass-independent isotope effects in planetary atmospheres and the early Solar system, Science, 283, 341–345, 1999.

ACPD
13, 9443–9483, 2013

Thiemens, M. H. and Heidenreich III, J. E.: The mass-independent fractionation of oxygen: a novel isotope effect and its possible cosmochemical implications, Science, 219, 1073–1075, 1983.
Thiemens, M. H. and Jackson, T.: Production of isotopically heavy ozone by ultraviolet light photolysis of oxygen, Geophys. Res. Lett., 14, 624–627, 1987.
Thiemens, M. H. and Jackson, T.: Pressure dependency for heavy isotope enhancement in ozone formation, Geophys. Res. Lett., 17, 717–719, 1990.
Tuzson, B. and Janssen, C.: Unambiguous identification of ^{17}O containing ozone isotopomers for symmetry selective detection, Isoto. Envir. Health Stud., 42, 67–75, 2006.
Vandenende, D. and Stolte, S.: The influence of the orientation of the NO molecule upon the chemi-luminescent reaction NO + $O_3 \rightarrow NO_2^*$+ O_2, Chem. Phys., 89, 121–139, 1984.
Vandenende, D., Stolte, S., Cross, J. B., Kwei, G. H., and Valentini, J. J.: Evidence for 2 different transition-states in the reaction of NO + $O_3 \rightarrow NO_2$+O_2, J. Chem. Phys., 77, 2206–2208, 1982.
Vicars, W. C., Bhattacharya, S. K., Erbland, J., and Savarino, J.: Measurement of the ^{17}O excess of tropospheric ozone using a nitride-coated filter, Rapid. Comm. Mass Spectrom., 26, 1219–1231, 2012.

ACPD
13, 9443–9483, 2013

NO_x cycle and tropospheric ozone isotope anomaly

G. Michalski et al.

Table 1. Oxygen isotopic composition of NO_2 modified by ozone in a NOx cycle experiment where the O-atom is supplied by dissociation of NO_2 by UV (Leighton cycle) with O_2 pressure at 500 torr and exposure time of 60 min.The δ values are relative to the tank oxygen in ‰ to express enrichment. The model values are obtained using coefficients 1.35 and 1.25 for formation of OOQ and OOP as discussed in the text. Predicted ozone δ values (in ‰) are : 84.7 ($\delta^{17}O$), 95.2 ($\delta^{18}O$) and 35.2 ($\Delta^{17}O$) in close agreement with enrichment of 86.0, 96.6 and 35.8 obtained by interpolation using data from Guenther et al. (1999) and Mauersberger et al. (2003).

Sample	NO_2 (µmole)	O_2 (µmole)	Ratio NO_2/O_2	Exptal values $\delta^{17}O$	$\delta^{18}O$	$\Delta^{17}O$ **	Model values $\delta^{17}O$	$\delta^{18}O$	$\Delta^{17}O$
Ozone d-values (published data and model values)				86.0	96.6	35.8	84.7	95.2	35.2
1	236.0	5.5E+05	4.3E-04	27.3	24.7	14.4	31.6	32.9	14.5
2	177.0	5.5E+05	3.2E-04	35.8	35.5	17.4	36.6	37.5	17.1
3	150.9	5.5E+05	2.8E-04	38.0	36.7	19.0	39.5	40.1	18.7
4	118.0	5.5E+05	2.2E-04	45.9	45.3	22.3	44.0	44.2	21.0
5	89.7	5.5E+05	1.6E-04	51.0	50.8	24.5	48.9	48.6	23.7
6	59.0	5.5E+05	1.1E-04	62.0	63.5	29.0	55.9	54.9	27.4
7	37.4	5.5E+05	6.8E-05	72.5	75.5	33.2	62.8	61.0	31.0
9	16.8	5.5E+05	3.1E-05	73.7	69.2	37.8	74.1	71.4	37.0

Tank Oxygen δ values: −5.69 and −10.84 in ‰ relative to VSMOW.
** $\Delta^{17}O = \delta^{17}O–0.52*\delta^{18}O$ measures the magnitude of mass independent enrichment.

ACPD
13, 9443–9483, 2013
NOx cycle and tropospheric ozone isotope anomaly
G. Michalski et al.

Table 2. Oxygen isotopic composition of NO_2 modified by ozone formed by UV in presence of oxygen with O-atom supplied by dissociation of NO_2 (Leighton cycle); the δ values show enrichment relative to Tank Oxygen in ‰. Model values are calculated by KINTECUS with coefficients chosen for ^{18}O and ^{17}O asymmetric ozone formation to match the observed values of isotopic enrichment as given in Table 3.

Sample	NO_2 (µmole)	Oxygen (torr)	O_2 (µmole)	Ratio NO_2/O_2	Experiment $\delta^{17}O$	Experiment $\delta^{18}O$	Experiment $\Delta^{17}O$	Model $\delta^{17}O$	Model $\delta^{18}O$	Model $\Delta^{17}O$
1	19.5	50	5.5E+04	3.6E-04	12.4	18.3	2.9	9.8	13.8	2.6
2	19.5	75	8.2E+04	2.4E-04	16.6	19.9	6.2	14.8	18.4	5.2
3	20.4	100	1.1E+05	1.9E-04	25.8	30.2	10.1	20.3	23.2	8.2
4	19.5	150	1.6E+05	1.2E-04	36.1	38.7	16.0	33.5	35.0	15.3
5	20.4	200	2.2E+05	9.3E-05	51.3	56.6	21.9	43.2	43.9	20.4
6	20.4	300	3.3E+05	6.2E-05	64.7	67.1	29.7	60.4	59.4	29.5
7	19.5	400	4.4E+05	4.5E-05	75.1	76.6	35.3	72.3	69.3	36.3
8	19.5	500	5.5E+05	3.6E-05	77.6	77.5	37.3	76.8	74.3	38.2
9	20.4	600	6.6E+05	3.1E-05	78.1	75.7	38.7	78.5	77.0	38.4
10	20.4	700	7.7E+05	2.7E-05	83.6	81.9	41.0	78.7	77.8	38.3
11	21.0	750	8.2E+05	2.6E-05	87.1	86.5	42.1	78.1	76.8	38.2
12	21.0	750	8.2E+05	2.6E-05	86.2	86.5	41.3	78.1	76.8	38.2
13	21.0	750	8.2E+05	2.6E-05	79.8	79.6	38.4	78.1	76.8	38.2
Mean	20	*750*	*Mean*		*84.4*	*84.2*	*40.6*	*sdev = 1.9*		

Chamber size is 20 liter and exposure time is 30 min.
Tank Oxygen δ values: −5.69 ($\delta^{17}O$) and −10.84 ($\delta^{18}O$) in ‰ relative to VSMOW.
$\Delta^{17}O = \delta^{17}O - 0.52 \cdot \delta^{18}O$ measures the extent of mass independent enrichment.

ACPD
13, 9443–9483, 2013

NOx cycle and tropospheric ozone isotope anomaly

G. Michalski et al.

Table 3. Typical number of molecules of reactants at the end of the chemical simulation for 60 min in the reaction chamber.

O_2 Pressure torr	NO_2 µmole	OO	OOO	O	ONO	NO
50 torr	20	1.64E+18	6.71E+09	4.76E+07	2.21E+13	5.52E+14
750 torr	20	2.46E+19	5.67E+11	4.77E+06	4.25E+14	1.47E+14
750 torr	236	2.46E+19	3.94E+11	4.68E+07	4.91E+15	2.16E+15

ACPD
13, 9443–9483, 2013

Table 4. Description of oxygen species used in the Kintecus chemical reaction model to simulate the NOx-O_3 cycling experiment (O = ^{16}O, P = ^{17}O, Q = ^{18}O). It is assumed that three major species constitute close to 100 % and other minor species can be neglected. δ values are relative to VSMOW in ‰.

Species	Isotope $\delta^{18}O$	ratios $d^{17}O$	Relative abundances
VSMOW	0	0	
O			0.9976200
P			0.0003790
Q			0.0020000
Total			0.9999990
Tank O_2 (bath gas)	−10.84	−5.69	
OO			0.9952457
OP			0.0007519
OQ			0.0039472
Total			0.9999448
Starting NO_2	−2.26	−1.25	
ONO			0.9952457
PNO			0.0007553
QNO			0.0039813
Total			0.9999822

ACPD
13, 9443–9483, 2013

NO$_x$ cycle and tropospheric ozone isotope anomaly

G. Michalski et al.

ACPD

13, 9443–9483, 2013

NO$_x$ cycle and tropospheric ozone isotope anomaly

G. Michalski et al.

Table 5. Adopted rate constants of reactions involving isotopomers of the species taking part in photolysis of NO_2 in presence of oxygen at 50 torr.

Reaction	Rate constant	Factor	Ref.
NO_2 dissociation			
ONO → O + NO	4.00E-03	j_1	assumed
PNO → P + NO	2.00E-03	$0.5\cdot j_1$	assumed
PNO → O + NP	2.00E-03	$0.5\cdot j_1$	assumed
QNO → Q + NO	2.00E-03	$0.5\cdot j_1$	assumed
QNO → O + NQ	2.00E-03	$0.5\cdot j_1$	assumed
Oxygen isotope exchange			
Q + OO → O + OQ	2.90E-12	k_0	1
O + OQ →Q + O_2	1.34E-12	$0.5\cdot k_0\cdot 0.924$	1
P + OO → O + OP	2.90E-12	k_0	1
O + OP → P + O2	1.39E-12	$0.5\cdot k_0\cdot 0.959$	1
Ozone formation			
O + OO + M → OOO + M	6.00E-34	k_1	2
O + OQ + M → OOQ + M	4.35E-34	$1.450\cdot k_1\cdot 0.5$	2
O + OQ + M → OQO + M	3.24E-34	$1.08\cdot k_1\cdot 0.5$	2
Q + OO + M → OOQ + M	5.52E-34	$0.92\cdot k_1$	2
Q + OO + M → OQO + M	3.60E-36	$0.006\cdot k_1$	2
O + OP +M → OOP + M	4.01E-34	$1.335\cdot k_1\cdot 0.5$	2
O + OP + M → OPO + M	3.12E-34	$1.04\cdot k_1\cdot 0.5$	2
P + OO + M → OOP + M	6.00E-34	$1.00\cdot k_1$	2
P + OO + M → OPO + M	3.60E-36	$0.006\cdot k_1$	2
Ozone dissociation			
OOO → O + OO	1.00E-06	j_2	assumed
OOP → P + OO	4.94E-07	$0.988\cdot j_2\cdot 0.5$	1
OOP → O + OP	5.00E-07	$0.5\cdot j_2$	1
OPO → O + OP	9.88E-07	$0.988\cdot j_2\cdot 0.5$	1
OOQ → Q + OO	4.86E-07	$0.972\cdot j_2\cdot 0.5$	1
OOQ → O + OQ	5.00E-07	$0.5\cdot j_2$	1
OQO → O + OQ	9.72E-07	$0.972\cdot j_2$	1
NO oxidation			
NO + OOO → ONO + OO	2.00E-14	k_2	3
NO + OOQ → ONO + OQ	1.00E-14	$0.5\cdot k_2$	assumed
NO + OOQ → QNO + OO	1.00E-14	$0.5\cdot k_2$	assumed
NO + OOP → ONO + OP	1.00E-14	$0.5\cdot k_2$	assumed
NO + OOP → PNO + OO	1.00E-14	$0.5\cdot k_2$	assumed
NO + OQO → ONO + OQ	2.00E-14	k_2	assumed
NO + OPO → ONO + OP	2.00E-14	k_2	assumed
NP + OOO → PNO + OO	2.00E-14	k_2	assumed
NQ + OOO → QNO + OO	2.00E-14	k_2	assumed
NO oxidation by O-atom			
O + NO + M → ONO + M	9.00E-32	k_3	3
Q + NO + M → QNO + M	9.00E-32	k_3	assumed
P + NO + M → PNO + M	9.00E-32	k_3	assumed
O + NP + M → PNO + M	9.00E-32	k_3	assumed
O + NQ + M → QNO + M	9.00E-32	k_3	assumed
NO_2 reaction with O-atom			
O+ ONO → NO + OO	1.00E-11	k_4	4
Q+ ONO → NO + OQ	9.57E-12	$k_4\cdot 0.957$	assumed
P+ ONO → NO + OP	9.78E-12	$k_4\cdot 0.978$	assumed
O+ PNO → NP + OO	5.00E-12	$0.5\cdot k_4$	assumed
O+ PNO → NO + OP	5.00E-12	$0.5\cdot k_4$	assumed
O+ QNO → NQ + OO	5.00E-12	$0.5\cdot k_4$	assumed
O+ QNO → NO + OQ	5.00E-12	$0.5\cdot k_4$	assumed
NO2 exchange with O-atom			
Q + ONO → O + QNO	2.09E-11	k_5	4
O + QNO → Q + ONO	9.57E-12	$0.5\cdot k_5/1.0923$	5
P + ONO → O + PNO	2.09E-11	k_5	assumed
O + PNO → P + ONO	9.96E-12	$0.5\cdot k_5/1.0487$	5
NO exchange with O-atom			
Q + NO → O + NQ	4.00E-11	k_6	6
O + NQ → Q + NO	3.63E-11	$(1/1.1017)\cdot k_6$	5
P + NO → O + NP	4.00E-11	k_6	assumed
O + NP → P + NO	3.80E-11	$(1/1.0536)\cdot k_6$	5
NO_2 exchange with NO			
NQ + ONO → QNO + NO	3.60E-14	k_7	7
NO + QNO → ONO + NQ	1.80E-14	$0.5\cdot k_7$	assumed
NP + ONO → PNO + NO	3.60E-14	k_7	assumed
NO + PNO → ONO + NP	1.80E-14	$0.5\cdot k_7$	assumed
NO oxidation by O_2			
NO+NO+OO → ONO+ONO	2.00E-38	k_8	8
NO+NQ+OO → ONO+QNO	2.00E-38	k_8	assumed
NO+NP+OO → ONO+PNO	2.00E-38	k_8	assumed
NO+NO+OQ → ONO+QNO	2.00E-38	k_8	assumed
NO+NO+OP → ONO+PNO	2.00E-38	k_8	assumed

[1] Pandey and Bhattacharya (2006); [2] Janssen et al. (2001); [3] Sander et al., JPL Publication 06-2 (2006); [4] Jaffe and Klein (1966); [5] Richet et al. (1977); [6] Anderson et al. (1985); [7] Lyons (2007); [8] Finlayson Pitts and Pitts (1999).

Table 6. The δ values of ozone relative to the source oxygen as obtained from Guenther et al. (1999) and Mauersberger et al. (2003) at various pressures of oxygen. The two coefficients for asymmetric ozone formation as a function of pressure are also given and they are chosen such that the model predicted δ values match the experimental values within 1 ‰.

Pressure	^{17}O-coeff* r^{17}	^{18}O-coeff* r^{18}	Experiment** δ^{17}O	Experiment** δ^{18}O	Experiment** Δ^{17}O***	Model δ^{17}O	Model δ^{18}O	Model Δ^{17}O
50	1.335	1.450	112.5	128.0	45.9	112.5	128.0	46.0
75	1.322	1.427	108.0	120.0	45.6	108.3	120.4	45.7
100	1.313	1.413	105.0	115.0	45.2	105.3	115.8	45.1
150	1.297	1.395	100.0	110.0	42.8	100.1	109.9	42.9
200	1.282	1.382	95.3	105.4	40.5	95.2	105.6	40.2
300	1.270	1.370	91.5	101.2	38.8	91.2	101.8	38.3
400	1.263	1.360	89.2	98.9	37.8	89.0	98.5	37.7
500	1.252	1.352	86.0	96.6	35.8	85.4	95.9	35.5
600	1.245	1.347	82.7	94.4	33.6	83.1	94.3	34.0
700	1.235	1.340	79.4	92.2	31.5	79.8	92.0	31.9
750	1.230	1.335	78.7	91.2	31.3	78.1	90.4	31.1

* Coefficient r^{17} equals the rate ratio (O+OP+M→OOP+M)/(O+OO+M→OOO+M) and a similar definition for coefficient r^{18}.
** The experimental values used for fitting are taken from Guenther et al. (1999) and Mauersberger et al. (2003).
*** Δ^{17}O= δ^{17}O-0.52*δ^{18}O measures the magnitude of mass independent enrichment.

ACPD
13, 9443–9483, 2013
NO$_x$ cycle and tropospheric ozone isotope anomaly
G. Michalski et al.

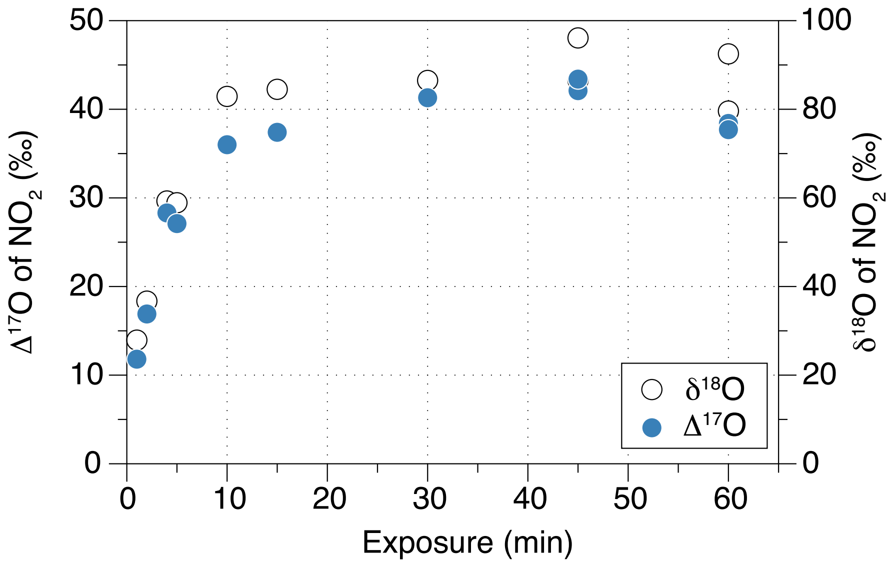

Fig. 1. The time scale for NO_x to achieve isotopic equilibrium in $\delta^{18}O$ and $\Delta^{17}O$ is approximately 30 min based on NO_x cycling experiment run with NO_2/O_2 ratio of $23 \cdot 10^{-6}$ (23 ppmv) at O_2 pressure of 750 torr in 20 L chamber.

ACPD
13, 9443–9483, 2013

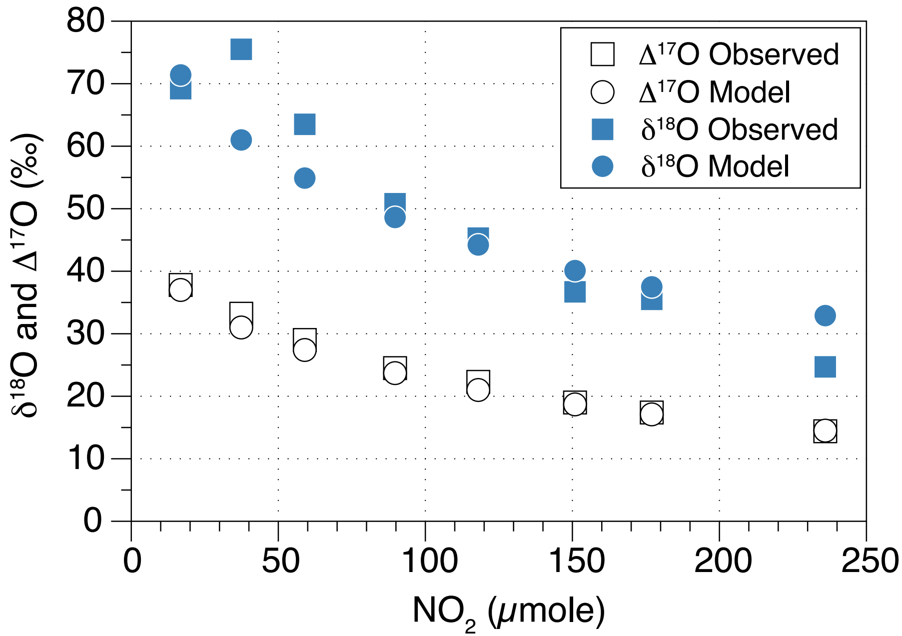

Fig. 2. Change in the steady state δ^{18}O and Δ^{17}O values of NO_2 as function of NO_2 amount as a result of photochemical cycling at O_2 pressure of 500 torr. Isotopic exchange between O and NO_x suppresses the δ values at high NO_2 concentration as seen by close agreement with the model predictions (see text for details).

ACPD
13, 9443–9483, 2013

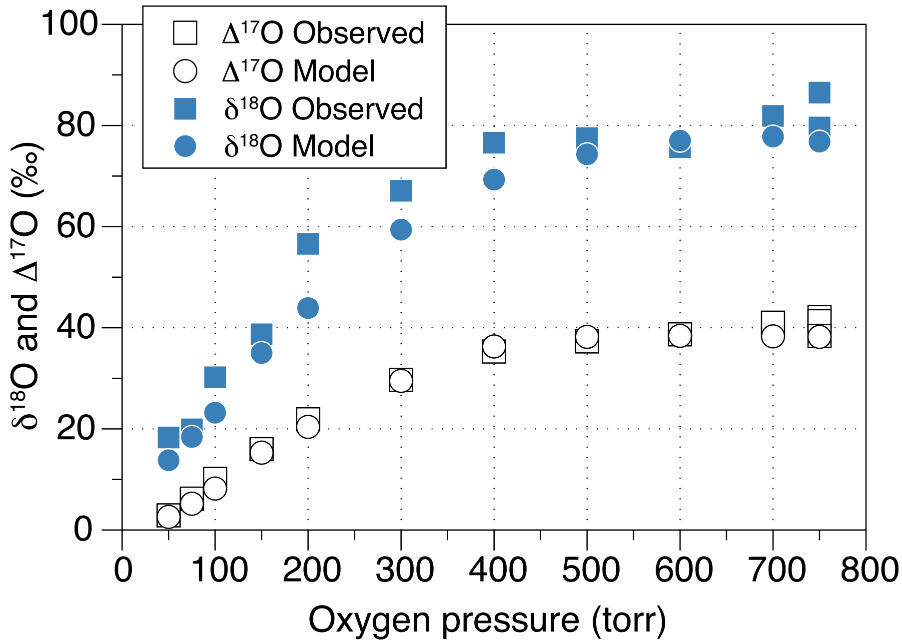

Fig. 3. Change in δ values of NO_2 as a result of photochemical cycling achieved with 20 µmole of NO_2 at oxygen pressures ranging from 50 to 750 torr in a 20 L photolysis chamber. As the O_2 pressure increases the ozone formation rate increases imparting higher enrichment to NO_2.

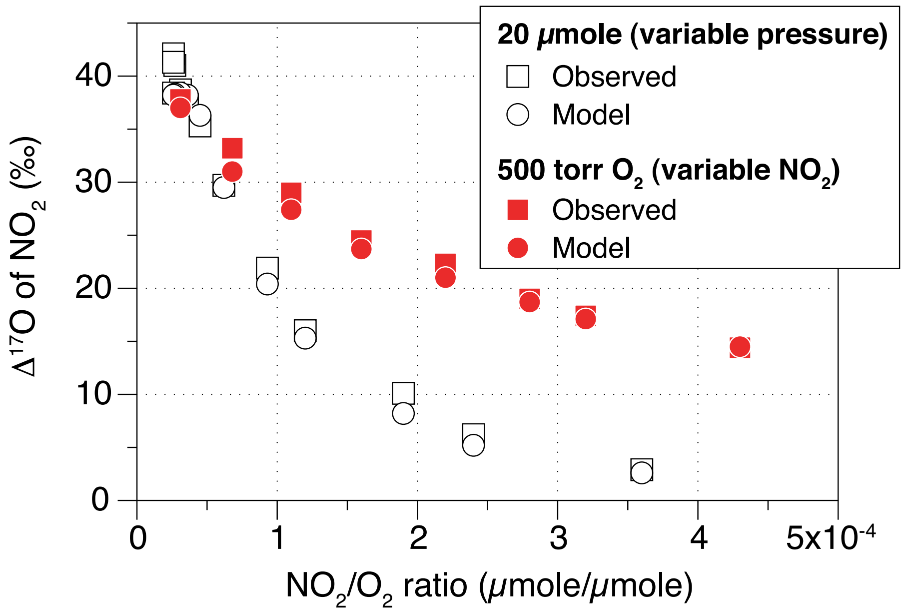

Fig. 4. $\Delta^{17}O$ of NO_2 based on all data obtained (from Table 1 and Table 2) plotted jointly as a function of NO_2/O_2 mixing ratio. As the NO_2 mixing ratio decreases, the $\Delta^{17}O$ values increase until they remain constant at a value of about 40 ‰ when the NO_2 mixing-ratio reaches about 20 ppmv (true for both curves). At the same mixing ratio, but higher O_2 pressure, the ozone formation rate increases resulting in more ozone oxidation of NO and larger $\Delta^{17}O$ values in the product NO_2 (the upper curve).

ACPD
13, 9443–9483, 2013

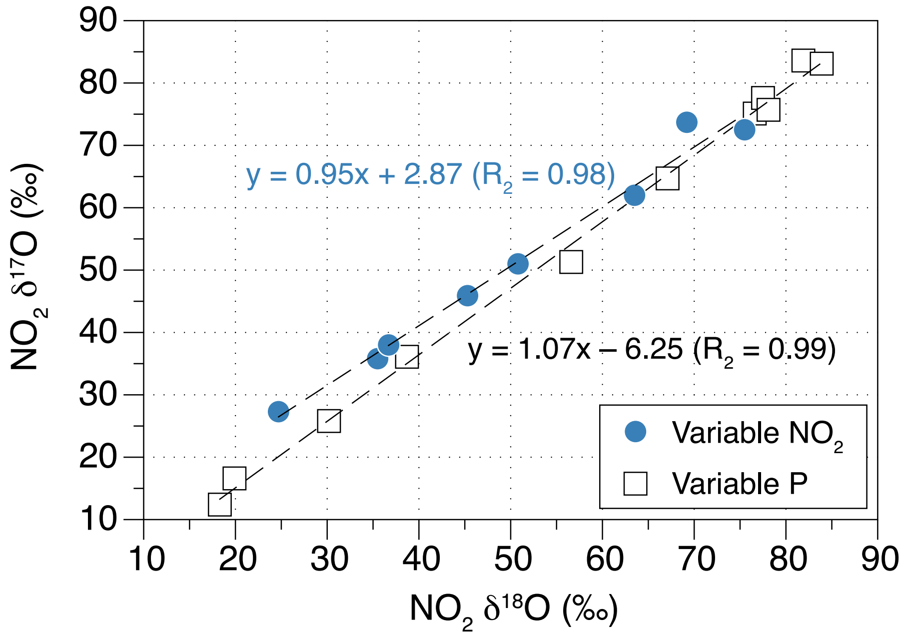

Fig. 5a. $\delta^{17}O$ versus $\delta^{18}O$ of NO_2 obtained after photochemical recycling in presence of oxygen. The blue circles correspond to points obtained by changing the NO_2 amount from 20 to 236 µmole while keeping the oxygen pressure constant at 50 torr. The boxes correspond to the case when NO_2 is kept constant at 20 µmole while the O_2 pressure is changed from 50 to 750 torr. The points in both sets align nearly along a line of slope 1 reflecting the progressive transfer of ozone isotopic ratios to NO_2. "Variable NO_2"-points reflect the same slope as ozone points experimentally obtained by other workers (see Fig. 5b).

ACPD
13, 9443–9483, 2013

NO$_x$ cycle and tropospheric ozone isotope anomaly

G. Michalski et al.

Title Page
Abstract | Introduction
Conclusions | References
Tables | Figures
◄ | ►
Back | Close
Full Screen / Esc
Printer-friendly Version
Interactive Discussion

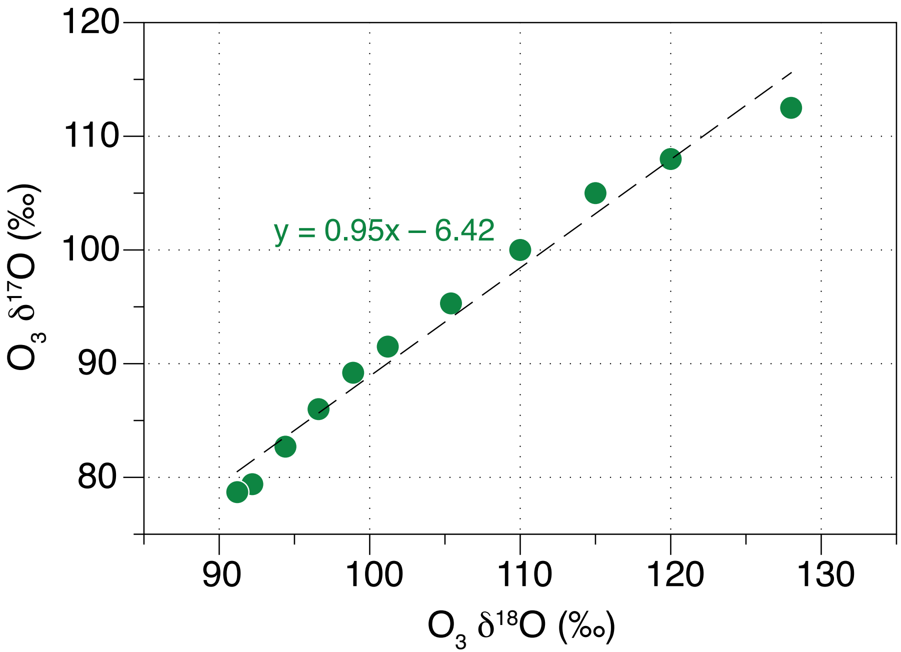

Fig. 5b. Ozone $\delta^{17}O$ versus ozone $\delta^{18}O$ plot showing a line of slope nearly unity (0.95) which intersects the y-axis at −6.42. The slope and intersect are reflected in the line through the NO_2 points shown by boxes in Fig. 5a indicating simple transfer of mass independent oxygen atoms to NO_2 by terminal atom reaction between ozone of variable $\Delta^{17}O$ enrichments and NO.

ACPD
13, 9443–9483, 2013

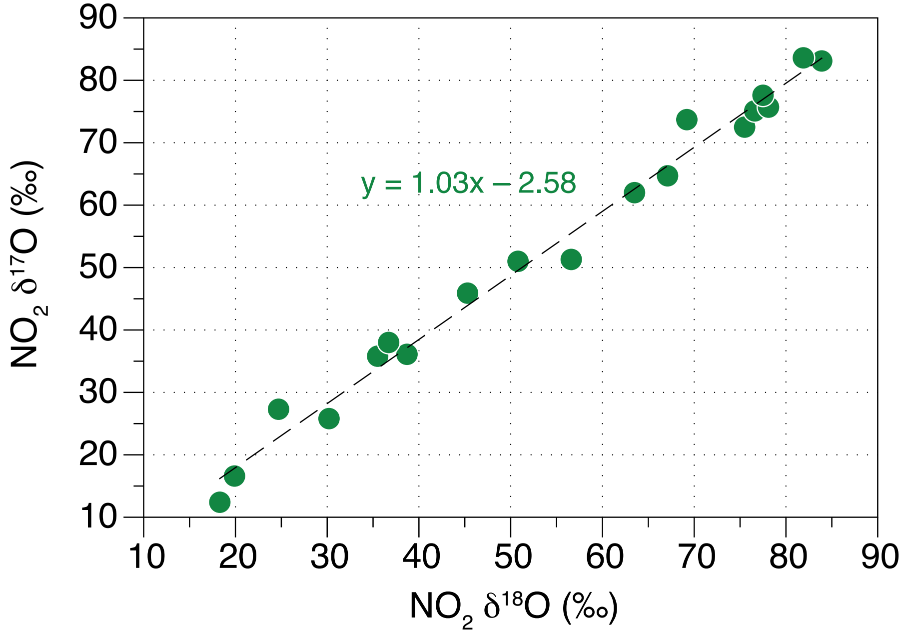

Fig. 5c. Combined plot of all NO_2 experimental points including both data sets shown in Fig. 5a.

ACPD
13, 9443–9483, 2013

NO_x cycle and tropospheric ozone isotope anomaly

G. Michalski et al.

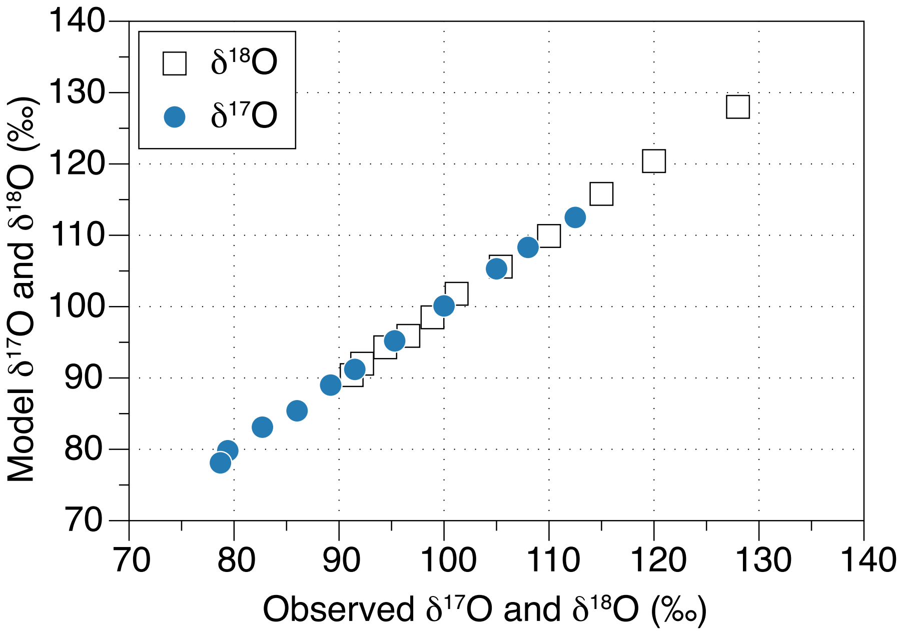

Fig. 6. The coefficients of asymmetric ozone production rate are chosen such that the delta values of ozone as obtained by interpolation from plots given by Guenther et al. (1999) and Mauersberger et al. (2003) are matched by the model predictions (see Table 5) within 0.8 ‰.

ACPD
13, 9443–9483, 2013

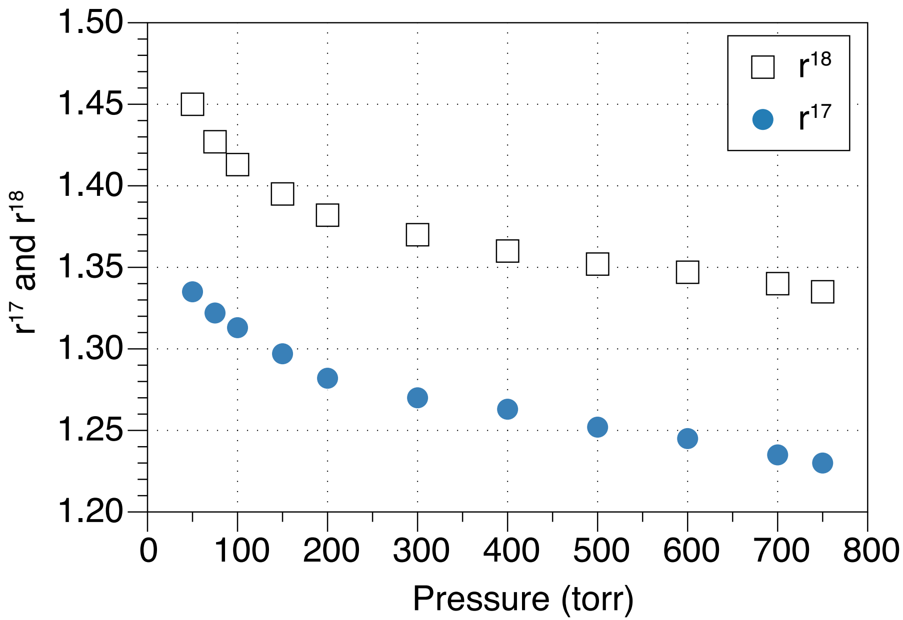

Fig. 7. Variation of rate coefficient ratios of asymmetric heavy ozone formation (relative to formation of OOO) as a function of pressure. r^{18} and r^{17} denote ratios of formation by O+OQ+M→OOQ and O+OP+M→OOP respectively. These values are used in the kintecus model and were chosen by trial and error method such that the δ values of ozone as obtained from published experimental results are reproduced closely (see Fig. 6).

ACPD
13, 9443–9483, 2013

NO$_x$ cycle and tropospheric ozone isotope anomaly

G. Michalski et al.

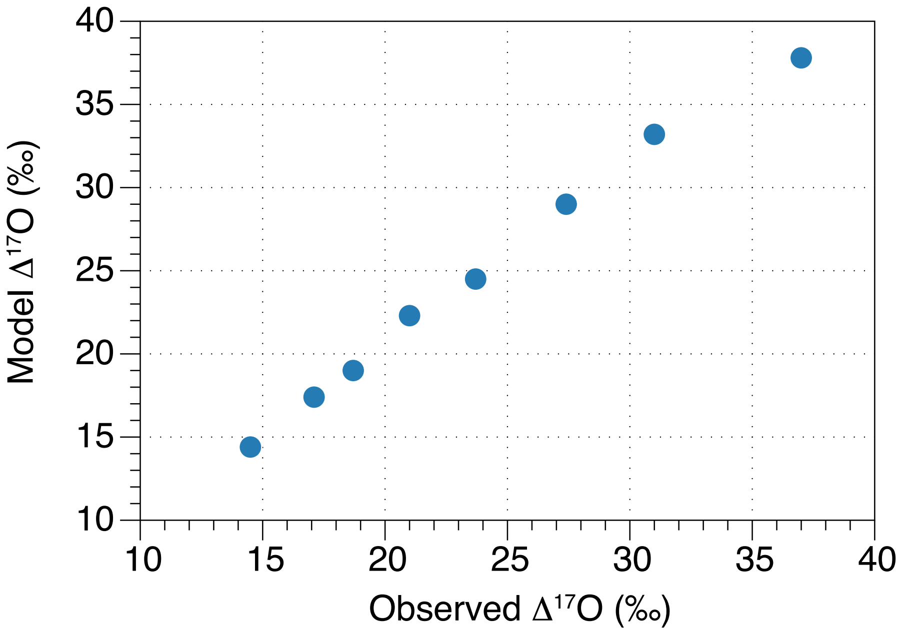

Fig. 8. This figure shows that the model $\Delta^{17}O$ values of NO_2 agree with observed values within 0 to 1.6 per mil with the choices of rate coefficients of ozone production in Table 5 (also in Fig. 7) confirming their validity.

Discussion Paper | Discussion Paper | Discussion Paper | Discussion Paper |

ACPD
13, 9443–9483, 2013

NO$_x$ cycle and tropospheric ozone isotope anomaly

G. Michalski et al.